ARTICLE
Journal of Cellular Biochemistry 112:2454–2462 (2011)

Journal of Cellular Biochemistry

Matrix Metalloproteinase-1 Induces Cleavage of Exogenous AlphaB-Crystallin Transduced by a Cell-Penetrating Peptide

Seung Won Yang,[1,2] Seung-Min Lee,[3] Eun Young Choi,[2,4,5] Kyung Hye Lee,[2,4,5] Soo Hyuk Kim,[2,4,5] Min-Jeong Shin,[3] Ye Sun Han,[6] Seok-Min Kang,[2,4,5] and Ji Hyung Chung[2,4,5*]

[1] *Department of Oral Histology and Developmental Biology & Program of Cell and Developmental Biology, School of Dentistry and Dental Research Institute, Seoul National University, Seoul 110-749, Korea*

[2] *Graduate Program in Science for Aging & Yonsei Research Institute of Aging Science, Yonsei University, Seoul 120-749, Korea*

[3] *Institute of Health Science & Department of Food and Nutrition, College of Health Science, Korea University, Seoul 136-703, Korea*

[4] *Severance Integrative Research Institute for Cerebral and Cardiovascular Diseases (SIRIC), Yonsei University Health System, Seoul 120-752, Korea*

[5] *Cardiovascular Research Institute, Yonsei University College of Medicine, Seoul 120-752, Korea*

[6] *Department of Advanced Technology Fusion, Konkuk University, Seoul 143-701, Korea*

ABSTRACT

Cell-penetrating peptides (CPPs), including TAT-CPP, have been used to deliver exogenous proteins into living cells. Although a number of proteins fused to TAT-CPP can be delivered into various cells, little is known about the proteolytic cleavage of TAT-fusion proteins in cells. In this study, we demonstrate that a small heat shock protein (sHSP), alphaB-crystallin (αB-crystallin), delivered by TAT-CPP is susceptible to proteolytic cleavage by matrix metalloproteinase-1 (MMP-1) in cardiac myoblast H9c2 cells. Recombinant TAT-αB-crystallin was efficiently transduced into H9c2 cells. For a few hours following protein transduction, generation of a 14-kDa fragment, a cleavage band of TAT-αB-crystallin, increased in a time-dependent manner. This fragment was observed only in detergent-insoluble fractions. Interestingly, treatment with MMP inhibitors blocked the cleavage of TAT-αB-crystallin. In test tubes, recombinant MMP-1 processed TAT-αB-crystallin to generate the major cleavage fragment 14-kDa, as observed in the cells treated with TAT-αB-crystallin. The N-terminal sequences of the 14-kDa fragment were identified as Leu-Arg-Ala-Pro-Ser-Trp-Phe, indicating that this fragment is generated by cleavage at Phe54-Leu55 of αB-crystallin. The MMP-1-selective inhibitor abolished the production of 14-kDa fragments in cells. In addition, the cleaved fragment of TAT-αB-crystallin was significantly reduced in cells transfected with MMP-1 siRNA. Moreover, the enzymatic activity of MMP-1 was markedly increased in TAT-αB-crystallin-treated cells. TAT-αB-crystallin has a cytoprotective effect on H9c2 cells under hypoxic insult, moreover, MMP-1-selective inhibitor treatment led to even increased cell viability. These results suggest that MMP-1 is responsible for proteolytic cleavage of TAT-αB-crystallin during its intracellular transduction in H9c2 cells. J. Cell. Biochem. 112: 2454–2462, 2011.

KEY WORDS: ALPHAB-CRYSTALLIN; CELL-PENETRATING PEPTIDE; MMP-1; PROTEOLYSIS

HSPs, which are expressed in response to various biological stresses such as heat, high pressure, and toxic agents, are a family of abundant cellular proteins. Based on their subunit molecular weight and sequence homology, they can be categorized into several classes [Richter et al., 2010]. Among them, sHSP family is generally classified by the ones with a molecular weight less than 30-kDa. It has been demonstrated that sHSPs have biological roles in protection of cells against a range of cellular stresses including

All authors including these two authors agreed to correct.
Grant sponsor: NRF, MEST (Korea); Grant number: 2009-0075206.
*Correspondence to: Ji Hyung Chung, PhD, Severance Integrative Research Institute for Cerebral and Cardiovascular Diseases (SIRIC), Yonsei University Health System, Seoul 120-752, Korea. E-mail: jhchung@yonsei.ac.kr
Received 19 January 2011; Accepted 22 April 2011 • DOI 10.1002/jcb.23167 • © 2011 Wiley-Liss, Inc.
Published online 2 May 2011 in Wiley Online Library (wileyonlinelibrary.com).

oxidative stress. The sHSP family is also involved in protein folding and the maintenance of protein homeostasis [Jiao et al., 2005; Sun and MacRae, 2005].

The αB-crystallin is a member of the small heat shock proteins and is abundant in the lens, followed by other non-lens tissues such as heart, skeletal muscle, and kidney [Dubin et al., 1989; Graw, 1997]. The molecular chaperon roles by αB-crystallin have been implicated in myopathy and cardiomyopathy [Vicart et al., 1998]. Previously, elevated expression of αB-crystallin in transgenic mouse model showed resistance to ischemia reperfusion injury-induced cell death, indicating its protective effect on the survival of cardiomyocyte [Ray et al., 2001]. Studies of cardiac cells as well as ischemic/reperfusion animal models suggest that overexpression of αB-crystallin using viral vectors confers a substantial protective effect [Ray et al., 2001; Morrison et al., 2004; Kadono et al., 2006]. However, for clinical applications of target genes including αB-crystallin, there is a concern regarding the use of plasmid transfection and viral infection due to undesired side effects such as acute syndrome and activation of the host's immune response [Ilies et al., 2002].

Cell-penetrating peptides (CPPs), also known as protein transduction domains, are small peptides less than 30 amino acids in length that can freely cross cellular membranes and enables the delivery of target molecules into cells [Morris et al., 2001; Chugh et al., 2010]. Among CPPs, TAT peptide from HIV-1 Tat protein which is comprised of 11 amino acids in length has been utilized to deliver target proteins into a variety of cells [Gump and Dowdy, 2007; Rapoport and Lorberboum-Galski, 2009]. Also TAT-CPP has been tried to deliver exogenous macromolecule into living animals and has recently shown promise in novel strategies for developing therapeutic proteins [Fonseca et al., 2009; Dietz, 2010]. Recombinant TAT-fusion proteins in denatured forms appear to be efficiently transduced and to be rapidly refolded inside of the cells [Becker-Hapak et al., 2001; Potocky et al., 2003; Richard et al., 2003]. One of the disadvantages of protein transduction using CPPs is that CPP-fusion proteins have a limited half-life in cells [Vives et al., 2008]. CPP-fusion proteins are rapidly eliminated following delivery by protease activities and renal clearance during systemic circulation [Torchilin and Lukyanov, 2003]. TAT-CPP is known to be cleaved by furin and other proteases [Tikhonov et al., 2004; Chauhan et al., 2007].

Although there is evidence for the cleavage site of the TAT-CPP sequence, little is known about the proteolytic cleavage of cargo proteins fused to TAT-CPP during TAT-mediated protein transduction. The present study demonstrated that αB-crystallin was successfully delivered by TAT-CPP to cardiac myoblast H9c2 cells. Once in the cells TAT-αB-crystallin becomes susceptible to proteolytic cleavage by MMP-1. The cleavage occurs in the internal target site of αB-crystallin in the fusion protein, producing a 14-kDa insoluble fragment.

MATERIALS AND METHODS

ANTIBODIES AND REAGENTS

Restriction enzymes were purchased from NEB (Ipswich, MA). Anti-αB-crystallin antibody was obtained from Stressgen, ENZO Life Sciences (Plymouth Meeting, PA). Anti-His-Tag antibody was purchased from Cell Signaling (Beverly, MA). Recombinant MMP-1 protein was purchased from R&D Systems (Minneapolis, MN). MMP-3, MMP-7, MMP-8, and MMP-9 recombinant proteins were obtained from ProSpec (Rehovot, Israel). Cell-permeable MMP inhibitors (GM1489, MMP-2 inhibitor, MMP-3 inhibitor, MMP-8 inhibitor, MMP-9 inhibitor) and the broad-spectrum MMP inhibitor III were purchased from Calbiochem (San Diego, CA). Other broad-spectrum MMP inhibitors including batimastat, marimastat, and Z-VAD-FMK were obtained from Tocris (Ellisville, MO). Anti-MMP-1 antibody was procured from Abbiotec (San Diego, CA). Anti-β-actin antibody, MG-132, cycloheximide, and chemical reagents were purchased from Sigma-Aldrich (St. Louis, MO).

CONSTRUCTION OF TAT-αB-CRYSTALLIN

The αB-crystallin fragment was amplified by PCR using the human heart cDNA library (BD Biosciences, Palo Alto, CA) as a template and PCR primers 5′-CACCTAGAATTCATGGACATCGCCATCCAC-3′ (upstream primer, the underlining indicates the *Eco*RI site) and 5′-AAGAAACTCGAGCTATTTCTTGGGGGCTGC-3′ (downstream primer, the underlining indicates the *Xho*I site). The αB-crystallin fragment was inserted into the *Eco*RI and *Xho*I sites of the pHis/TAT vector [Kwon et al., 2007] for TAT-αB-crystallin fusion protein expression. Another αB-crystallin fragment (*Nde*I and *Xho*I sites) was also inserted into the corresponding sites of the pET28a vector (Novagen, Madison, WI) for preparation of αB-crystallin without the TAT domain. To construct the TAT-αB-crystallin-His_6, which contains His-Tag at the C-terminus of the TAT-αB-crystallin, the PCR reaction was performed using the following downstream primer: 5′-AAGAAACTCGAGCTAGTGATGATGATGATGATGTTTC-TTGGGGGCTGC-3′ (the underlining indicates the *Xho*I site). Plasmid constructs were confirmed by both restriction enzyme mapping and DNA sequence analyses.

EXPRESSION AND PURIFICATION OF THE TAT-αB-CRYSTALLIN PROTEIN

E. coli BL21 (DE3) (Novagen) transformed with recombinant plasmids was grown in LB broth at 37°C. Protein expression was induced by the addition of 1 mM IPTG for 4 h. The bacterial pellet was harvested by centrifugation and resuspended in buffer Z (8 M urea, 100 mM NaCl, and 20 mM HEPES, pH 8.0). The clarified lysate was loaded onto a Ni-NTA affinity column (Qiagen, Hilden, Germany). His-tagged proteins were eluted with a linear gradient from 100 mM to 1 M imidazole in buffer. The proteins were loaded onto a PD-10 desalting column to facilitate rapid exchange to the PBS. The recombinant proteins were further purified using endotoxin-removing gel (Pierce, Rockford, IL). The purified fusion protein was assessed by 12.5% SDS-PAGE and Coomassie blue staining.

CELL CULTURE AND PROTEIN TRANSDUCTION INTO CELLS

The rat heart-derived myoblast cell line, H9c2, was obtained from the American Type Culture Collection (ATCC, Rockville, MD) and was cultured in DMEM/F-12 supplemented with 10% FBS. For intracellular transduction of the TAT-αB-crystallin protein, cells were grown to confluence in culture dishes. The culture medium was

replaced with fresh medium containing 10% FBS and was then treated with the TAT-αB-crystallin protein. The cells were washed with PBS and treated with trypsin-EDTA for 5 min. They were then washed with PBS and analyzed with several biochemical assays.

IMMUNOBLOT ANALYSIS

Protein-treated cells were washed with PBS and lysed in a lysis buffer (Cell Signaling, Beverly, MA). Protein concentrations were determined using the Bradford protein assay kit (BioRad, Hercules, CA). Proteins resolved on SDS-polyacrylamide gel were transferred onto polyvinylidene difluoride (PVDF) membranes (Millipore, Bedford, MA). The membranes were blocked overnight at 4°C with 5% nonfat dried milk in TBS-T (TBS with 0.05% Tween-20) and then incubated with primary antibodies, followed by incubation with horseradish peroxidase-conjugated secondary antibodies. Protein bands were detected using the enhanced chemiluminescence (ECL) reagent (Santa Cruz Biotechnology, Santa Cruz, CA).

PREPARATION OF DETERGENT-INSOLUBLE FRACTION

After cells were lysed with a lysis buffer, samples were centrifuged at 4°C, and the supernatants were collected as soluble fraction. The remaining pellet was washed twice with PBS and resuspended in urea lysis buffer (8 M urea, 4% CHAPS, and 10 mM Tris-Cl, pH 7.4) for 1 h at 4°C. The samples were centrifuged and the supernatant was used as the detergent-insoluble fraction.

IMMUNOCYTOCHEMISTRY

Cells treated with proteins on 4-well plastic dishes (SonicSeal Slide, Nalge Nunc, Rochester, NY) were washed with PBS and then fixed with methanol and ethanol (1:1 ratio) for 10 min. The cells were washed again with PBS and then treated with PBS containing 0.2% triton for 15 min. The cells were treated with PBS containing 5% BSA and then incubated with anti-His-Tag-Alexa 647 conjugate (Invitrogen, Carlsbad, CA) for 1 h. For nuclear staining, DAPI (0.02 μg/ml final concentration) was added to the cells. After washing with PBS, the cells staining patterns were visualized by confocal microscopy (LSM 510 META, Carl Zeiss, Thornwood, NY).

MMP REACTIONS AND N-TERMINAL SEQUENCING

The recombinant TAT-αB-crystallin (10 μg) was incubated with active MMPs (0.25 μg) in cleavage buffer (50 mM Tris-Cl, pH 7.5, 3 mM NaN_3, 5 mM $CaCl_2$, and 1 μM $ZnCl_2$) for 2 h at 37°C. Proteolytic fragments of TAT-αB-crystallin with MMP-1 were subjected to a SDS-PAGE gel and then transferred to a PVDF membrane (Millipore). Following staining with Coomassie blue, the corresponding band was subjected to Edman degradation and sequenced in a Procise 491 protein sequencer (Applied Biosystems, Foster City, CA) at the Korea Basic Science Institute (KBSI, Seoul, Korea).

MMP-1 SIRNA TRANSFECTION

MMP-1 siRNA oligonucleotides targeting the sequences, 5′-GATCAAGTCCGCTATTTCA-3′ and 5′-GGTTCTACATTCGTGTAAA-3′, were purchased from Genolution Pharmaceuticals (Seoul, Korea). Cells were transfected with a pool of two MMP-1 siRNAs (5 nM each) using Lipofectamine RNAiMAX (Invitrogen). Following 24 h of transfection, the level of MMP-1 was analyzed with anti-MMP-1 antibody. A scrambled siRNA-A (Santa Cruz Biotechnology) was used as the control.

MMP-1 ACTIVITY ASSAY

The activity of MMP-1 was determined using the SensoLyte 520 MMP-1 Fluorimetric Assay Kit (AnaSpec, Fremont, CA). Briefly, cell lysates were added to each microplate well, which was precoated with anti-MMP-1 antibody. After MMP-1 was pulled down, the MMP-1 fluorogenic substrate 5-FAM (fluorophore) and QXL520 (quencher)-labeled fluorescence resonance energy transfer (FRET) peptide were added to the well. After 1 h of treatment with 1 mM of *p*-aminophenylmercuric acetate, the fluorescence intensity was measured at 490/520 nm (excitation/emission) wavelength.

CELL VIABILITY AND APOPTOSIS ASSAY

Cell viability was determined by the trypan blue dye exclusion method. Cells were washed with PBS and harvested from dishes with 0.1% trypsin and neutralized by adding FBS. They were then centrifuged and the cell pellet was resuspended in PBS. Following the addition of an equal volume of 0.4% trypan blue in PBS, the percentage of blue cells was counted by scoring 250 cells with a hemocytometer. Cells per well were counted in triplicate. Terminal deoxynucleotidyl transferasemediated dUTP nick end-labeling (TUNEL) analysis was performed with a commercially available kit according to the manufacturer's instructions (Invitrogen). The caspase-3 activity was determined using a Caspase-3 Colorimetric Assay Kit (Millipore).

STATISTICAL ANALYSIS

Data are expressed as means ± SE. Statistical comparisons were performed by one-way analysis of variance and Student's *t*-test. Differences were considered significant at $P < 0.05$.

RESULTS

TRANSDUCTION OF THE TAT-αB-CRYSTALLIN INTO H9C2 CELLS

The recombinant TAT-αB-crystallin protein was expressed in *E. coli* and purified using Ni-NTA affinity column chromatography. The purified TAT-αB-crystallin protein was nearly homogeneous and >95% pure, as determined by SDS-PAGE analysis with Coomassie blue staining (Fig. 1a). Using the same methods, the recombinant αB-crystallin protein without the TAT domain was also purified as a control. The identities of the recombinant proteins were confirmed by SDS-PAGE and immunoblot analysis with the anti-αB-crystallin antibody recognizing the C-terminal epitope of the αB-crystallin (Fig. 1b). To check the transduction of the recombinant proteins to the rat cardiac myoblast H9c2 cells, their localization after 1 h treatment in the cells were examined using immunocytochemistry analysis.

This analysis revealed that the TAT-αB-crystallin was efficiently transduced into the cells, whereas the αB-crystallin without the TAT domain was not taken up (Fig. 1c). The intracellular transduction of the TAT-αB-crystallin was also confirmed by immunoblot analysis using the anti-His-Tag antibody (Fig. 1d, left blot) and the anti-αB-crystallin antibody (Fig. 1d, right blot). TAT-αB-crystallin was

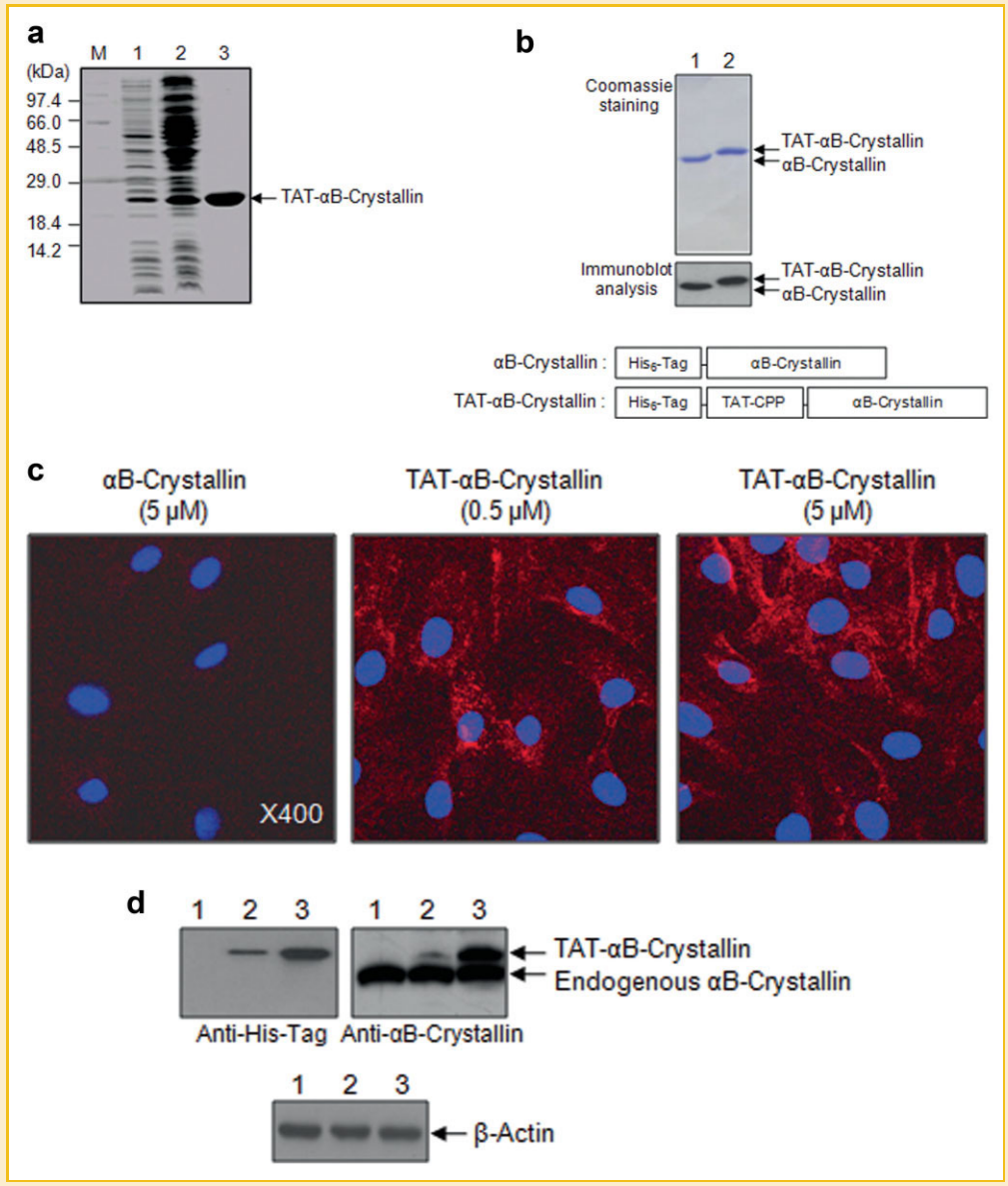

Fig. 1. Purification and intracellular transduction of the TAT-αB-crystallin protein. a: The TAT-αB-crystallin protein was purified by Ni-NTA affinity and PD-10 desalting column chromatography. The products of each step were analyzed by SDS-PAGE and Coomassie blue staining. Lane M, molecular weight markers; lane 1, before IPTG-induction; lane 2, after IPTG-induction; lane 3, fraction eluted from Ni-NTA affinity column. b: The αB-crystallin proteins fused with or without TAT-CPP were analyzed by SDS-PAGE and immunoblot assay using anti-αB-crystallin (upper panel). Lane 1, αB-crystallin; lane 2, TAT-αB-crystallin. The lower panel shows a schematic representation of the recombinant proteins. c: H9c2 cells were treated with αB-crystallin or TAT-αB-crystallin proteins for 1 h and stained with anti-His-Tag-Alexa 647 and DAPI. Protein transduction was observed using confocal microscopy. d: H9c2 cells were treated with recombinant proteins for 1 h. Immunoblot analysis was performed with anti-His-Tag or anti-αB-crystallin antibodies. Lane 1, αB-crystallin (5 μM); lane 2, TAT-αB-crystallin (0.5 μM); lane 3, TAT-αB-crystallin (5 μM).

transduced into cells in a concentration-dependent manner. In addition, endogenous αB-crystallin was not changed following the intracellular transduction of recombinant TAT-αB-crystallin (Fig. 1d, right blot).

CLEAVAGE OF TRANSDUCED TAT-αB-CRYSTALLIN IN CELLS

During intracellular transduction of the TAT-αB-crystallin, we observed the appearance of a novel 14-kDa band, which was recognized by anti-αB-crystallin antibody. This band intensity was increased in a time-dependent manner (Fig. 2a). The 14-kDa fragment was not shown in the control cells, which was not treated with TAT-αB-crystallin. As anti-αB-crystallin antibody recognizes the C-terminal epitope, this 14-kDa product is likely to be a proteolytic C-terminal product derived from the TAT-αB-crystallin. When the cells were incubated with other TAT-fusion proteins, such as TAT-EGFP and TAT-survivin as controls, there were no other smaller proteolytic fragments observed by their respective specific antibodies (data not shown). When cells were treated with the TAT-αB-crystallin-His_6 protein containing the His-Tag at the C-terminus of the TAT-αB-crystallin, the 14-kDa fragment could be detected by

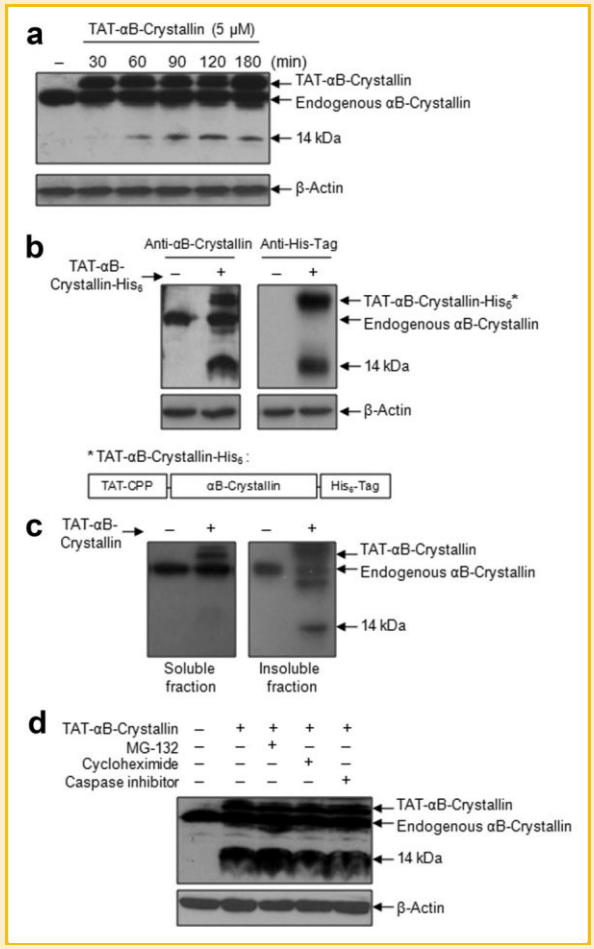

Fig. 2. Cleavage of the TAT-αB-crystallin transduced into H9c2 cells. a: H9c2 cells were treated with 5 μM of TAT-αB-crystallin and harvested at the indicated times. Whole cell lysates were immunoblotted with anti-αB-crystallin antibody. b: H9c2 cells were treated with 5 μM of TAT-αB-crystallin-His_6 for 3 h. Whole cell lysates were immunoblotted with anti-αB-crystallin or anti-His-Tag antibodies. The lower panel shows a schematic representation of the TAT-αB-crystallin-His_6 protein. c: H9c2 cells were treated with 5 μM of TAT-αB-crystallin for 3 h. The soluble and insoluble fractions from cell lysates were analyzed by immunoblot assay using anti-αB-crystallin antibody. d: H9c2 cells were pretreated with MG-132 (10 μM), cycloheximide (10 μg/ml), or pan-caspase inhibitor (Z-VAD-FMK, 50 μM) for 1 h. The cells were then treated with 5 μM of TAT-αB-crystallin for 3 h. Whole cell lysates were analyzed by immunoblot assay using anti-αB-crystallin antibody.

an anti-His-Tag antibody, whereas endogenous αB-crystallin was not detected (Fig. 2b). This indicates that the 14-kDa fragment is the result of processing from exogenous TAT-αB-crystallin, rather than a product of endogenous αB-crystallin or a nonspecific artifact. To gain an insight of whether a 14-kDa fragment is in the state of an active form, we examined the solubility of this truncated product. The soluble and insoluble fractions in a buffer containing nonionic detergent were analyzed by immunoblot assay, and the 14-kDa was only observed in the insoluble fraction (Fig. 2c), indicating that this fragment may not be an active form of αB-crystallin. In order to identify cellular factors involved in the cleavage of the TAT-αB-crystallin, we pretreated several inhibitors, such as MG-132 and pan-caspase inhibitors prior to the treatment of the TAT-αB-crystallin. However, we observed no significant changes in the 14-kDa fragment in the inhibitor-treated groups (Fig. 2d). In addition, treatment of a protein synthesis inhibitor, cycloheximide, did not affect the appearance of the 14-kDa fragment (Fig. 2d), therefore, ruling out the possibility of a new synthesized product of a truncated form of endogenous αB-crystallin.

CLEAVAGE OF THE TAT-αB-CRYSTALLIN BY MMP-1

Interestingly, cleavage of the TAT-αB-crystallin was blocked by pretreatment of cells with a broad-spectrum MMP inhibitor (MMP inhibitor III, Calbiochem) (Fig. 3a). The same results were obtained when the cells were treated with other MMP inhibitors, such as batimastat and marimastat (data not shown). After treatment with the MMP inhibitor, we observed a significant reduction in the 14-kDa fragments of TAT-αB-crystallin in the insoluble fraction (Fig. 3b).

Next, we tested the susceptibility of the TAT-αB-crystallin to proteolytic cleavage by recombinant MMPs in test tubes. Recombinant active MMPs were incubated with the TAT-αB-crystallin, and samples were separate by SDS-PAGE and subjected to Coomassie blue staining. As shown in Figure 4a, MMP-1 cleaved the TAT-αB-crystallin protein to generate a 14-kDa fragment, and cleavage products of similar size were also observed in the groups with MMP-8 or MMP-9. Immunoblot analysis confirmed that MMP-1 processed the TAT-αB-crystallin to generate the major cleavage fragment 14-kDa (Fig. 4b, right blot). This cleavage pattern of fragmentation by MMP-1 was the same as that observed in the cells treated with the TAT-αB-crystallin (Fig. 4b, left blot), indicating that MMP-1 may be involved in TAT-αB-crystallin cleavage in the cells. MMP-1 cleaved the TAT-αB-crystallin to a 14-kDa product in a time-dependent

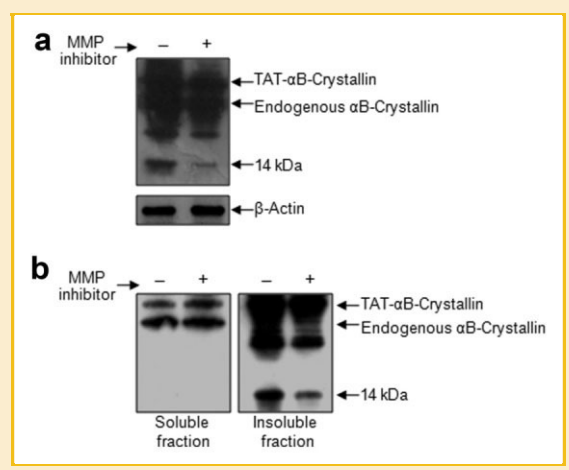

Fig. 3. Effect of the MMP inhibitor on the cleavage of the TAT-αB-crystallin. a: H9c2 cells were pretreated with 300 nM of a broad-spectrum cell-permeable MMP inhibitor for 1 h. The cells were then treated with 5 μM of TAT-αB-crystallin for 3 h. Whole cell lysates were analyzed by immunoblot assay using anti-αB-crystallin antibody. b: H9c2 cells pretreated with an MMP inhibitor were incubated with 5 μM of TAT-αB-crystallin for 3 h. The soluble and insoluble fractions were analyzed by immunoblot assay using anti-αB-crystallin antibody.

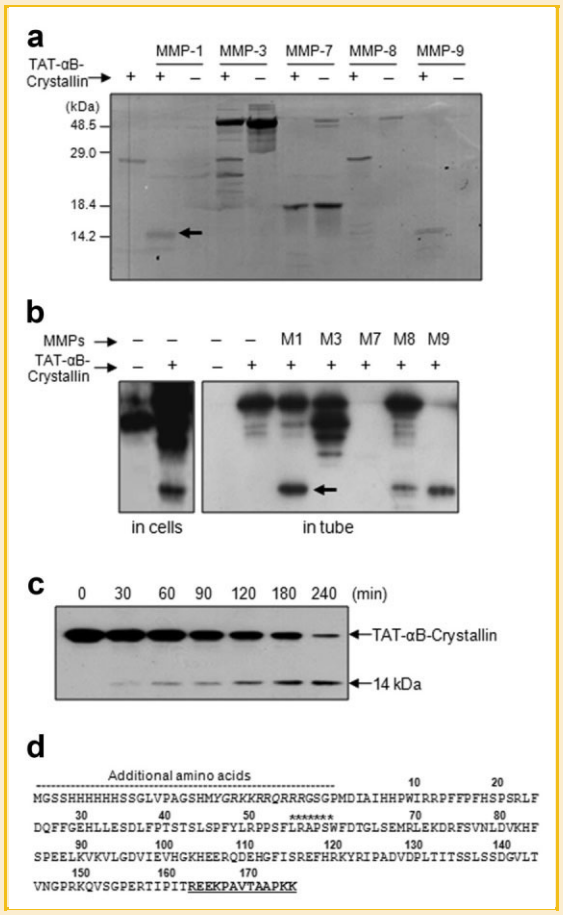

Fig. 4. Cleavage of TAT-αB-crystallin by MMP-1. a: The TAT-αB-crystallin was incubated with various MMPs for 2 h in test tubes. The cleavage patterns of the TAT-αB-crystallin were analyzed by SDS-PAGE and Coomassie blue staining. An arrow indicates the cleaved 14-kDa fragment. b: The cleavage patterns of the TAT-αB-crystallin were also assessed by immunoblot assay using anti-αB-crystallin antibody. An arrow indicates the cleaved 14-kDa fragment. c: The TAT-αB-crystallin was incubated with MMP-1 for various time periods. Cleavages of the TAT-αB-crystallin were analyzed by immunoblot assay using anti-αB-crystallin antibody. d: Illustration of the TAT-αB-crystallin cleaved by MMP-1. The reaction sample was separated by SDS-PAGE and then transferred to the PVDF membrane. The N-terminal sequence of the cleavage band was analyzed by an automatic amino-acid sequencer. The asterisks indicate the amino acids (Leu-Arg-Ala-Pro-Ser-Trp-Phe) that are identical to the result of N-terminal sequencing. The epitope of the anti-αB-crystallin antibody is underlined at the C-terminus of the αB-crystallin. Additional amino acids containing TAT-CPP at the N-terminus of the αB-crystallin are represented by the dotted line. Italic letters represent TAT-CPP.

manner (Fig. 4c), whereas the other MMPs were less efficient at cleaving this site of the TAT-αB-crystallin (data not shown). To determine the specific cleavage site of the TAT-αB-crystallin by MMP-1, the cleavage products were analyzed by SDS-PAGE and transferred to PVDF membranes. A 14-kDa band was excised, and N-terminal sequencing was conducted. The N-terminal sequences of the 14-kDa fragments of the TAT-αB-crystallin after the MMP-1 reaction were identified as Leu-Arg-Ala-Pro-Ser-Trp-Phe (LRAPSWF) (Fig. 4d). The predicted molecular weight of the 14-kDa fragment generated by cleavage at Phe54-Leu55 of the αB-crystallin was 13,713 Da, which is consistent with the size observed from SDS-PAGE.

SELECTIVE CLEAVAGE OF THE TAT-αB-CRYSTALLIN BY MMP-1 AND INTRACELLULAR MMP-1 ACTIVITY

As MMP-1 cleaved the TAT-αB-crystallin in test tube reactions (Fig. 4c) and the broad-spectrum MMP inhibitors blocked the generation of 14-kDa fragments in H9c2 cells (Fig. 3), we tested whether MMP-1 was specifically involved in TAT-αB-crystallin fragmentation in cells. Pretreating the cells with several MMP inhibitors revealed that the MMP-1-selective inhibitor (GM1489) abolished the production of 14-kDa fragments (Fig. 5a). The cleaved fragments of TAT-αB-crystallin also disappeared in the cells transfected with siRNA to induce the knockdown of MMP-1 (Fig. 5b). To check whether TAT-αB-crystallin transduction affected

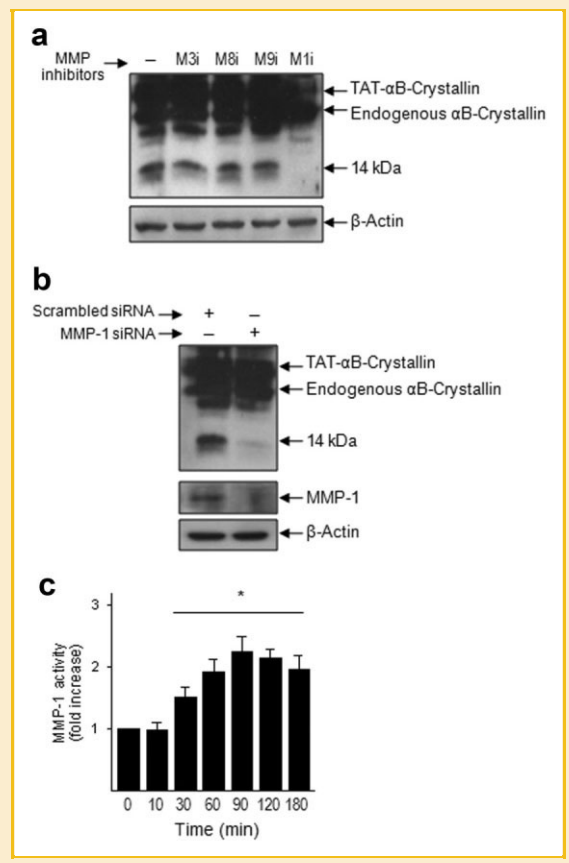

Fig. 5. Selective cleavage of the TAT-αB-crystallin by MMP-1 and intracellular MMP-1 activity. a: H9c2 cells were pretreated with specific inhibitors against MMPs (M1i, MMP-1 inhibitor, 20 nM; M3i, MMP-3 inhibitor, 0.5 μM; M8i, MMP-8 inhibitor, 100 nM; M9i, MMP-9 inhibitor, 50 nM) for 1 h. The cells were then treated with 5 μM of TAT-αB-crystallin for 3 h. Whole cell lysates were analyzed by immunoblot assay using anti-αB-crystallin antibody. b: H9c2 cells were transfected with MMP-1 siRNA. After 24 h, the cells were incubated with 5 μM of TAT-αB-crystallin for 3 h. Cell lysates were analyzed by immunoblot assay using anti-αB-crystallin antibody. c: H9c2 cells were incubated with 5 μM of TAT-αB-crystallin. At the indicated time points, MMP-1 activity was determined by an MMP-1 activity assay kit. $^{*}P < 0.05$ compared to control.

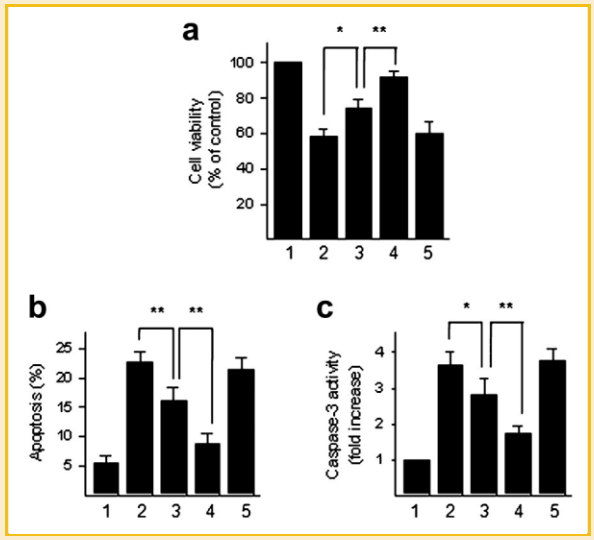

Fig. 6. Effect of MMP-1 on the cytoprotective activity of TAT-αB-crystallin. H9c2 cells were pretreated with 20 nM of MMP-1 inhibitor for 1 h. The cells were treated with 5 μM of TAT-αB-crystallin and then subjected to hypoxia for 24 h. a: Cell viability was assessed by the trypan blue dye exclusion method. b: Percent cells undergoing apoptosis are measured by the TUNEL assay. c: Caspase-3 activity was determined using caspase-3 assay kit. 1, Normoxia; 2, hypoxia; 3, hypoxia with 5 μM of TAT-αB-crystallin; 4, hypoxia with 5 μM of TAT-αB-crystallin, and 20 nM of MMP-1 inhibitor; 5, hypoxia with 20 nM of MMP-1 inhibitor. Data are averages of three independent experiments. $^{*}P < 0.05$, $^{**}P < 0.01$.

MMP-1 activity, we measured intracellular MMP-1 activity in the presence of lysate of TAT-αB-crystallin-treated cells. MMP-1 activity was significantly elevated after 30 min of TAT-αB-crystallin treatment (Fig. 5c), and there was a high correlation between cleavage of TAT-αB-crystallin (Fig. 2a) and MMP-1 activity.

EFFECT OF MMP-1 ON THE CYTOPROTECTIVE ACTIVITY OF TAT-αB-CRYSTALLIN

We showed that transduced TAT-αB-crystallin is cleaved by activated MMP-1 in H9c2 cells. We next investigated whether this increased activity of MMP-1 in TAT-αB-crystallin-treated cells might in turn decrease the intracellular cytoprotective capability of exogenous TAT-αB-crystallin. To assess the cytoprotective activity of TAT-αB-crystallin, we used an in vitro model of ischemia in which H9c2 cells are exposed to sustained hypoxia. As shown in Fig. 6a, after hypoxic insult for 24 h, the viability of H9c2 cells in the TAT-αB-crystallin-treated group was 73.9% (± 5.8), compared to 58.6% (± 4.1) in hypoxia control group. At this time, MMP-1-selective inhibitor treatment led to even increased cell viability; cell viability was greater than 90% with pretreatment of MMP-1-selective inhibitor. Similar results were obtained using the TUNEL assay (Fig. 6b) and caspase-3 activity assay (Fig. 6c).

DISCUSSION

In the present study, we demonstrated that MMP-1 induces cleavage of exogenous αB-crystallin transduced by CPP in cardiac cells. Most CPP-fusion proteins have been produced under denaturation conditions because many eukaryotic proteins expressed in bacterial expression systems are likely to form inclusion bodies. Moreover, the conformation of denatured CPP-fusion proteins may possibly be appropriate for effective intracellular transduction [Becker-Hapak et al., 2001; Potocky et al., 2003; Richard et al., 2003]. Most of the relevant literature reports that these CPP-fusion proteins are successfully delivered into cells. However, protein transduction strategies face various problems. In some cases, recombinant CPP-fusion proteins are not taken up by cells [Falnes et al., 2001; Yang et al., 2002]. Furthermore, even if cellular uptake is successfully attained, not all of the proteins are active inside the cells [Cashman et al., 2003; Sengoku et al., 2003] because protein transduction and its activity in cells may depend on cell type and the properties of the CPP-fusion proteins. Our results also showed that the 14-kDa fragments of TAT-αB-crystallin, which is probably the inactive form, were predominantly detected in detergent-insoluble fractions, whereas the full-length protein was present in both soluble and insoluble fractions (Fig. 2c). In addition, the decreased amount of 14-kDa fragments in the insoluble fractions following MMP inhibitor treatment coincided with an increase in the intensity of soluble, full-length TAT-αB-crystallin (Fig. 3b). When H9c2 cells were treated with a mutant TAT-αB-crystallin protein (55–175), which is same fragment as a proteolytic C-terminal product derived from the TAT-αB-crystallin by MMP-1 activity, this protein was detected only in detergent-insoluble fractions, which is probably the inactive form (data not shown). These data may support the idea that in some cases, such as during the accumulation of excessive exogenous proteins in cells, MMP is activated to cleave accumulated proteins, thereby localizing them into detergent-insoluble compartments as inactive fragments. Indeed, αB-crystallin is the most abundant sHSP constitutively expressed in cardiomyocytes and H9c2 cells [Kumarapeli and Wang, 2004; Mao et al., 2004].

In general, abnormal proteins, such as misfolded or unfolded proteins, as well as short-lived proteins in eukaryotic cells, are degraded by the ubiquitin–proteasome system [Dantuma and Lindsten, 2010]. The endoplasmic reticulum (ER) cellular stress response is also related to the unfolded protein response, which promotes the elimination of unfolded proteins [Rasheva and Domingos, 2009]. However, ER stress-marker proteins, such as the C/EBP homologous protein (CHOP) and BiP/GRP78 were not changed in cells transduced with TAT-αB-crystallin transduction (data not shown). In addition, the caspase inhibitor, proteasome inhibitor, or other protease inhibitors did not reduce the accumulation of 14-kDa fragments of TAT-αB-crystallin over the course of a few hours, although they might be degraded by the proteasome system after a longer period of protein transduction into cells. Unexpectedly, we found that the MMP-1 inhibitor blocks the generation of the 14-kDa fragments of TAT-αB-crystallin in cells. Cleaved fragments of TAT-αB-crystallin also disappeared in the cells transfected with MMP-1 siRNA. The 14-kDa fragment seems to be derived from proteolytic cleavage of exogenous TAT-αB-crystallin. As the cleavage was not affected by cycloheximide (Fig. 2d) and the 14-kDa fragment was detected by the His-Tag antibody in the TAT-αB-crystallin-His_6 protein-treated cells

(Fig. 2b), it is not an experimental artifact, a newly synthesized protein or a product of endogenous αB-crystallin. Furthermore, we did not observe the generation of 14-kDa fragments in the culture medium during TAT-αB-crystallin transduction into cells (data not shown). These observations strongly suggest that the intracellular action of MMP-1 controls the cleavage of exogenous TAT-αB-crystallin. Indeed, we detected a significant increase in MMP-1 activity in TAT-αB-crystallin-treated cells (Fig. 5c). Overall previous studies indicate that the protective role of αB-crystallin in the cardiac cells [Ray et al., 2001; Morrison et al., 2004; Kadono et al., 2006]. Moreover, αB-crystallin expression in the H9c2 cells is downregulated after hypoxia/ischemia insult [Lin et al., 2010]. Therefore our effort to supply additional αB-crystallin proteins to the cardiac cells was aimed to provide a protective mechanism against stress-induced cell death. In our hands TAT-αB-crystallin treatment significantly increased cell survival after hypoxic insult, besides, a greater-than-additive increase of cell viability was observed when combining a MMP-1 inhibitor with TAT-αB-crystallin (Fig. 6), suggesting that this synergy may be attributable to suppression of MMP-1 activity, thereby inhibiting TAT-αB-crystallin cleavage. Upon intracellular transduction of TAT-αB-crystallin, a significant protection against doxorubicin-induced cell death was also observed in MCF-7 cells with low αB-crystallin expression (data not shown). Further study is now underway to clarify the cleavage of TAT-αB-crystallin and its biological function in H9c2 cells which are deficient in αB-crystallin using knock-down method by siRNA transfection.

It has been reported that MMPs involved in the remodeling of the extracellular matrix are known to degrade the extracellular matrix molecules and membrane-bound proteins [Davis and Senger, 2008]. Recent evidence, however, has shown that MMPs are also found within cells and that they exert proteolytic actions on various intracellular substrates [Kwan et al., 2004; Limb et al., 2005; Dean and Overall, 2007; Butler and Overall, 2009; Cauwe et al., 2009]. Intracellular substrate proteolysis by MMPs activated in cells is also involved in pathological events associated with protein-conformational diseases such as cataracts, multiple sclerosis, cardiomyopathy, and Parkinson's disease [Cauwe and Opdenakker, 2010]. For instance, a study has demonstrated that αB-crystallin, known as the most abundant protein in early active multiple sclerosis lesions, is cleaved at multiple sites by MMP-9 [Starckx et al., 2003]. In addition, a recent report has shown that various MMPs induce cleavage of αB-crystallin at multiple sites [Shiryaev et al., 2009], including Phe54-Leu55, an MMP-1 cleavage site identified in our study (Fig. 4d). These observations strongly suggest that MMPs may be activated under various conditions, such as during the accumulation of exogenous proteins in cells and that they may exert distinct responses, including the cleavage of substrate proteins. Although additional studies are required to determine the mechanism of MMP-1 activation, our data may provide early insight into how exogenous CPP-fusion proteins are processed at an early stage following protein transduction in cells. Furthermore, the present study could open a route for improving the intracellular stability of exogenous proteins used therapeutically, given that transduced proteins have only a limited active half-life.

ACKNOWLEDGMENTS

This research was supported by Basic Science Research Program through the National Research Foundation of Korea (NRF) funded by the Ministry of Education, Science and Technology (Grant No. 2009-0075206).

REFERENCES

Becker-Hapak M, McAllister SS, Dowdy SF. 2001. TAT-mediated protein transduction into mammalian cells. Methods 24:247–256.

Butler GS, Overall CM. 2009. Updated biological roles for matrix metalloproteinases and new intracellular substrates revealed by degradomics. Biochemistry 48:10830–10845.

Cashman SM, Morris DJ, Kumar-Singh R. 2003. Evidence of protein transduction but not intercellular transport by proteins fused to HIV tat in retinal cell culture and *in vivo*. Mol Ther 8:130–142.

Cauwe B, Martens E, Proost P, Opdenakker G. 2009. Multidimensional degradomics identifies systemic autoantigens and intracellular matrix proteins as novel gelatinase B/MMP-9 substrates. Integr Biol (Camb) 1:404–426.

Cauwe B, Opdenakker G. 2010. Intracellular substrate cleavage: A novel dimension in the biochemistry, biology and pathology of matrix metalloproteinases. Crit Rev Biochem Mol Biol 45:351–423.

Chauhan A, Tikoo A, Kapur AK, Singh M. 2007. The taming of the cell penetrating domain of the HIV Tat: Myths and realities. J Control Release 117:148–162.

Chugh A, Eudes F, Shim YS. 2010. Cell-penetrating peptides: Nanocarrier for macromolecule delivery in living cells. IUBMB Life 62:183–193.

Dantuma NP, Lindsten K. 2010. Stressing the ubiquitin-proteasome system. Cardiovasc Res 85:263–271.

Davis GE, Senger DR. 2008. Extracellular matrix mediates a molecular balance between vascular morphogenesis and regression. Curr Opin Hematol 15:197–203.

Dean RA, Overall CM. 2007. Proteomics discovery of metalloproteinase substrates in the cellular context by iTRAQ labeling reveals a diverse MMP-2 substrate degradome. Mol Cell Proteomics 6:611–623.

Dietz GP. 2010. Cell-penetrating peptide technology to deliver chaperones and associated factors in diseases and basic research. Curr Pharm Biotechnol 11:167–174.

Falnes PO, Wesche J, Olsnes S. 2001. Ability of the Tat basic domain and VP22 to mediate cell binding, but not membrane translocation of the diphtheria toxin A-fragment. Biochemistry 40:4349–4358.

Dubin RA, Wawrousek EF, Piatigorsky J. 1989. Expression of the murine alpha B-crystallin gene is not restricted to the lens. Mol Cell Biol 9:1083–1091.

Fonseca SB, Pereira MP, Kelley SO. 2009. Recent advances in the use of cell-penetrating peptides for medical and biological applications. Adv Drug Deliv Rev 61:953–964.

Graw J. 1997. The crystallins: Genes, proteins and diseases. Biol Chem 378:1331–1348.

Gump JM, Dowdy SF. 2007. TAT transduction: The molecular mechanism and therapeutic prospects. Trends Mol Med 13:443–448.

Ilies MA, Seitz WA, Balaban AT. 2002. Cationic lipids in gene delivery: Principles, vector design and therapeutical applications. Curr Pharm Des 8:2441–2473.

Jiao W, Li P, Zhang J, Zhang H, Chang Z. 2005. Small heat-shock proteins function in the insoluble protein complex. Biochem Biophys Res Commun 335:227–231.

Kadono T, Zhang XQ, Srinivasan S, Ishida H, Barry WH, Benjamin IJ. 2006. CRYAB and HSPB2 deficiency increases myocyte mitochondrial permeability transition and mitochondrial calcium uptake. J Mol Cell Cardiol 40:783–789.

Kumarapeli AR, Wang X. 2004. Genetic modification of the heart: Chaperones and the cytoskeleton. J Mol Cell Cardiol 37:1097–1109.

Kwan JA, Schulze CJ, Wang W, Leon H, Sariahmetoglu M, Sung M, Sawicka J, Sims DE, Sawicki G, Schulz R. 2004. Matrix metalloproteinase-2 (MMP-2) is present in the nucleus of cardiac myocytes and is capable of cleaving poly (ADP-ribose) polymerase (PARP) *in vitro*. FASEB J 18:690–692.

Kwon JH, Kim JB, Lee KH, Kang SM, Chung N, Jang Y, Chung JH. 2007. Protective effect of heat shock protein 27 using protein transduction domain-mediated delivery on ischemia/reperfusion heart injury. Biochem Biophys Res Commun 363:399–404.

Limb GA, Matter K, Murphy G, Cambrey AD, Bishop PN, Morris GE, Khaw PT. 2005. Matrix metalloproteinase-1 associates with intracellular organelles and confers resistance to lamin A/C degradation during apoptosis. Am J Pathol 166:1555–1563.

Lin CH, Wu WS, Lin MT, Liu WP, Hsu RB, Chang CP. 2010. Attenuating ischemia-induced H9c2 myoblasts apoptosis by therapeutic hypothermia. Am J Med Sci 339:258–265.

Mao YW, Liu JP, Xiang H, Li DW. 2004. Human alphaA- and alphaB-crystallins bind to Bax and Bcl-X(S) to sequester their translocation during staurosporine-induced apoptosis. Cell Death Differ 11:512–526.

Morris MC, Depollier J, Mery J, Heitz F, Divita G. 2001. A peptide carrier for the delivery of biologically active proteins into mammalian cells. Nat Biotechnol 19:1173–1176.

Morrison LE, Whittaker RJ, Klepper RE, Wawrousek EF, Glembotski CC. 2004. Roles for alphaB-crystallin and HSPB2 in protecting the myocardium from ischemia-reperfusion-induced damage in a KO mouse model. Am J Physiol Heart Circ Physiol 286:H847–H855.

Potocky TB, Menon AK, Gellman SH. 2003. Cytoplasmic and nuclear delivery of a TAT-derived peptide and a beta-peptide after endocytic uptake into HeLa cells. J Biol Chem 278:50188–50194.

Rapoport M, Lorberboum-Galski H. 2009. TAT-based drug delivery system–new directions in protein delivery for new hopes? Expert Opin Drug Deliv 6:453–463.

Rasheva VI, Domingos PM. 2009. Cellular responses to endoplasmic reticulum stress and apoptosis. Apoptosis 14:996–1007.

Ray PS, Martin JL, Swanson EA, Otani H, Dillmann WH, Das DK. 2001. Transgene overexpression of alphaB crystallin confers simultaneous protection against cardiomyocyte apoptosis and necrosis during myocardial ischemia and reperfusion. FASEB J 15:393–402.

Richard JP, Melikov K, Vives E, Ramos C, Verbeure B, Gait MJ, Chernomordik LV, Lebleu B, 2003. Cell-penetrating peptides. A reevaluation of the mechanism of cellular uptake. J Biol Chem 278:585–590.

Richter K, Haslbeck M, Buchner J. 2010. The heat shock response: Life on the verge of death. Mol Cell 40:253–266.

Sengoku T, Bondada V, Hassane D, Dubal S, Geddes JW. 2003. Tat-calpastatin fusion proteins transducer primary rat cortical neurons but do not inhibit cellular calpain activity. Exp Neurol 188:161–170.

Shiryaev SA, Remacle AG, Savinov AY, Chernov AV, Cieplak P, Radichev IA, Williams R, Shiryaeva TN, Gawlik K, Postnova TI, Ratnikov BI, Eroshkin AM, Motamedchaboki K, Smith JW, Strongin AY. 2009. Inflammatory proprotein convertase-matrix metalloproteinase proteolytic pathway in antigen-presenting cells as a step to autoimmune multiple sclerosis. J Biol Chem 284: 30615–30626.

Starckx S, Van den Steen PE, Verbeek R, van Noort JM, Opdenakker G. 2003. A novel rationale for inhibition of gelatinase B in multiple sclerosis: MMP-9 destroys alpha B-crystallin and generates a promiscuous T cell epitope. J Neuroimmunol 141:47–57.

Sun Y, MacRae TH. 2005. Small heat shock proteins: Molecular structure and chaperone function. Cell Mol Life Sci 62:2460–2476.

Tikhonov I, Ruckwardt TJ, Berg S, Hatfield GS, Pauza CD. 2004. Furin cleavage of the HIV-1 Tat protein. FEBS Lett 565:89–92.

Torchilin VP, Lukyanov AN. 2003. Peptide and protein drug delivery to and into tumors: Challenges and solutions. Drug Discov Today 8:259–266.

Vicart P, Caron A, Guicheney P, Li Z, Prevost MC, Faure A, Chateau D, Chapon F, Tome F, Dupret JM, Paulin D, Fardeau M. 1998. A missense mutation in the alphaB-crystallin chaperone gene causes a desmin-related myopathy. Nat Genet 20:92–95.

Vives E, Schmidt J, Pelegrin A. 2008. Cell-penetrating and cell-targeting peptides in drug delivery. Biochim Biophys Acta 1786:126–138.

Yang Y, Ma J, Song Z, Wu M. 2002. HIV-1 TAT-mediated protein transduction and subcellular localization using novel expression vectors. FEBS Lett 532:36–44.